Bull Environ Contam Toxicol (2009) 83:455–461
DOI 10.1007/s00128-009-9743-3

Distribution of Polycyclic Aromatic Hydrocarbons and *n*-Alkanes in Surface Sediments from Shinano River, Japan

Tomiyuki Hori · Naoya Shiota · Takashi Asada · Kikuo Oikawa · Kuniaki Kawata

Received: 11 September 2008 / Accepted: 23 April 2009 / Published online: 8 May 2009

Abstract The distribution of polycyclic aromatic hydrocarbons (PAHs) and *n*-alkanes was investigated in the surface sediment from the Shinano River in Niigata, Japan. The total concentrations of the PAHs and *n*-alkanes ranged from 102 to 10,450 ng/g dry weight and from 160 to 3,530 ng/g dry, respectively. Perylene (Per) in the sediment samples originated from both the same anthropogenic sources as benzo[*a*]pyrene and the natural sources; the anthropogenically derived Per was estimated at 0.4%–27% of the Per in the sediment. The carbon preference index values ranged from 0.77 to 2.48, suggesting the differences in the *n*-alkane sources at the investigated sites. The investigated sites were divided into three clusters by the cluster analysis.

Keywords PAH · *n*-Alkane · Sediment · Distribution

Polycyclic aromatic hydrocarbons (PAHs) and *n*-alkanes distribute in the environment as ubiquitous contaminants (Cranwell and Koul 1989). The PAHs originate from the incomplete combustion of organic matter, the emissions of petrogenic products and the transformation of biogenic precursors. Although some PAHs, such as perylene, have biogenetic sources (Cranwell and Koul 1989; Kawata et al. 1997), most PAHs have anthropogenic sources. The anthropogenic PAHs mainly enter surface waters via atmospheric fallout, urban run-off, municipal effluents and oil spillage or leakage (Vrana et al. 2001). The *n*-alkanes originate from artificial sources, e.g., the biomass burning and the emissions of petroleum products, as well as natural sources, e.g., terrestrial vegetation and biogeneic. The PAHs and *n*-alkanes migrate from the surface water to the sediment because of their extremely low solubility in water. Therefore, sediment is the best media for evaluation of the impact of PAHs and *n*-alkanes on the water environment (Tareq et al. 2005). A number of studies have been performed on the distributions in river sediment of PAHs including the 16 PAHs listed as priority pollutants in Test Methods SW-846 by the US Environmental Protection Agency (Vrana et al. 2001); several papers have been published on the *n*-alkane distributions in river sediment (Ye et al. 2007).

The Shinano River is the longest river in Japan with a total length of 367 km. We have previously reported the distributions of four five-ring PAHs i.e., benzo[*a*]pyrene (BaP), benzo[*b*]fluoranthene (BbF), benzo[*k*]fluoranthene (BkF) and perylene (Per), and 29 compounds with two to four rings, including naphthalene (Nap), acenaphthylene (Acy), acenaphthene (Ace), fluorene (Flu), phenanthrene (Phe), anthracene (Ant), fluoranthene (Flt) and pyrene (Pyr), in the surface sediment from rivers in Niigata including the Shinano River (Kawata et al. 1997, 2005). The objective of this study was to assess the recent distribution of the common PAHs and Per as well as *n*-alkanes in the surface sediment from the Shinano River, and to identify their compositions for their potential sources. The target PAHs were Nap, Acy, Ace, Flu, Phe, Ant, Flt, Pyr, benz[*a*]anthracene (BaA), chrysene (Chr), benzo[*c*]phenanthrene (BcP), BbF/ benzo[*j*]fluoranthene/BkF (BFs),

T. Hori · N. Shiota · T. Asada · K. Oikawa · K. Kawata (✉)
Faculty of Applied Life Sciences, Niigata University of Pharmacy and Applied Life Sciences, 265-1 Higashijima, Akiha-ku, Niigata 956-8603, Japan
e-mail: kawata@nupals.ac.jp

Present Address:
T. Asada
Faculty of Symbiotic Systems Science, Fukushima University, 1 Kanayagawa, Fukushima, Fukushima 960-1296, Japan

BaP, Per, 3-methylcholanthrene (3Mc), dibenz[*a*,*h*]anthracene (DahA), indeno[1,2,3-*c*,*d*]pyrene (Inp) and benzo[*g*,*h*,*i*]perylene (BghiP). The target *n*-alkanes contain decane (C_{10}) to dotriacontane (C_{32}).

Materials and Methods

An ultrasonic processor VCX-130PD, 20 kHz and 130 W (Sonics & Materials, Newtown, CT), equipped with a titanium alloy probe (3 mm diameter), were used for extraction procedures. A Finnigan POLARIS Q gas chromatograph–ion trap mass spectrometer (Thermo Electron, Waltham, MA) equipped with a 30 m × 0.25 mm id (0.25 μm film thickness) fused-silica HPX-5 column (Agilent, Palo Alto, CA) was used for the quantitative analysis. The standard chemicals for the target compounds were purchased from Supelco (Bellefonte, PA). The other reagents were purchased from Wako (Osaka, Japan) and Kanto (Tokyo, Japan). Standard solutions, surrogate solutions and an internal standard solution (50 μg/mL) were prepared in acetone. A Varian Mega Bond Elut Si (Palo Alto, CA) was washed with 10 ml of dichloromethane prior to use.

Sediment samples were collected at 14 sites from the Shinano River in Niigata Prefecture, Japan (Fig. 1) from November 2005 to April 2006. The sediment samples were stored at 5°C in the dark, and were extracted within 48 h after collection. The organic content (Table 1) was estimated as the loss upon ignition (550°C, 15 h) and calculated as percent dry weight (Kawata et al. 2005). The extraction procedure is as follows. Surrogate compounds (5 μg each) were added to 50 g of a sediment sample, and then the sample was added to a 50 mL portion of acetone. To the mixture was added 10 mL of dichloromethane and then ultrasonicated for 10 min. The slurry was next centrifuged at 3,000 rpm (1,700×*g*) for 10 min. This supernatant solvent phase was filtered through a glass-fiber filter. The extraction procedure was repeated twice. The extracts were combined and washed three times with 50 mL of purified water. After the organic layer was dried over anhydrous sodium sulfate, 100–250 mg of copper powder was added to the solution by shaking to remove the sulfur. The resulting solution was concentrated to about 5 mL by an evaporator and then to 1 mL under a purified nitrogen gas stream. The obtained solution was placed in a silica gel cartridge and eluted with 30 mL of dichloromethane (fraction 1), and subsequently with 50 mL of dichloromethane–acetone (95 + 5, v/v) solution (fraction 2). Each of eluate was condensed to 1 mL. A 1 μg internal standard solution was added to each of the concentrated solutions for GC/MS determination. The GC/MS conditions were as follows: column temperature programmed from 50°C (held for 2 min) to 290°C (held for 60 min) at 5°C/min, injector temperature 250°C, injection mode splitless, helium carrier gas flowrate 1.0 mL/min, MS transfer temperature 290°C, ion source temperature 250°C, ionization mode electron impact, ionization energy 70 eV. The quantification ions were 128 for Nap, 152 for Acy, 154 for Ace, 166 for Ful, 178 for Phe and Ant, 202 for Flt and Pyr, 228 for BaA and Chr, 228 for BcP, 252 for BFs, 252 for BaP and Per, 268 for 3Mc, 276 for Inp, 278 for DahA, 276 for BghiP, 57 and

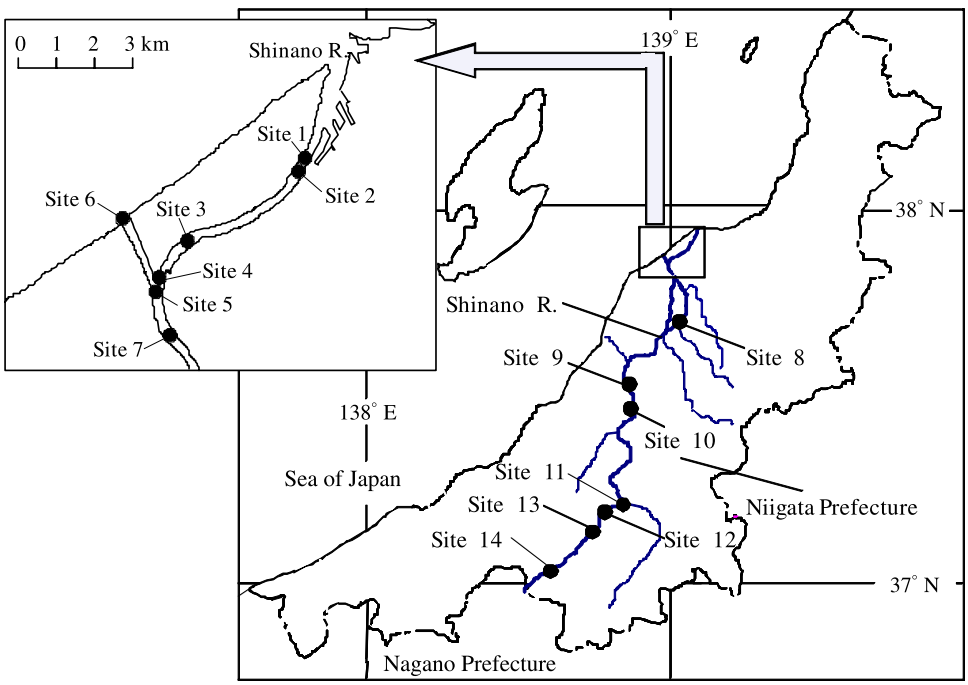

Fig. 1 Sampling sites

Table 1 PAH concentrations in sediments of the Shinano River

Compound	Abbr.	Concentration (ng/g dry)							
		Site 1	Site 2	Site 3	Site 4	Site 5	Site 6	Site 7	Site 8
Naphthalene	Nap	5.3	0.6	3.2	1.0	7.3	1.7	0.6	0.8
Three-ring PAHs		145	17.8	28.7	10.3	61.1	77.0	16.0	16.6
Acenaphthylene	Acy	5.0	1.2	5.7	2.8	2.7	16	0.6	0.2
Acenaphthene	Ace	12.2	0.4	<0.1	<0.1	1.2	<0.1	0.5	0.3
Fluorene	Flu	15.4	1.1	<0.1	<0.1	3.7	<0.1	1.0	0.9
Phenanthrene	Phe	81.8	13.3	7.1	<0.1	49	47	12	14
Anthracene	Ant	30	2.0	16	7.5	4.9	13.8	1.5	0.9
Four-ring PAHs		1,930	130	80.9	11.9	97.7	125	100	67.5
Fluoranthene	Flt	314	32	24	2.1	41	60.6	27	15
Pyrene	Pyr	311	26	17	<0.1	28	51.6	21	22
Benz[*a*]anthracene	BaA	41.1	<0.3	1.9	<0.3	2.1	<0.3	<0.3	1.7
Chrysene	Chr	570	25	27	6.8	9.8	2.1	17	6.9
Benzo[*c*]phenanthrene	BcP	690	46	11	3.0	16	10	36	23
Five-ring PAHs[a]		3,220	123	93	40	44	6.0	84	236
Benzo[*b*]fluoranthene + Benzo[*j*]fluoranthene + Benzo[*k*]fluoranthene	BFs	674	46	20	6.2	10	3.0	39	57
Benzo[*a*]pyrene	BaP	1,634	33	29	8.0	15	3.0	22	26
3-Methylcholanthrene	3Mc	226	31	28	17	<0.8	<0.8	3.0	60
Dibenz[*a,h*]anthracene	DahA	692	13	16	9.1	18	<0.7	20	93
Perylene	Per	981	160	35	11	26	19	168	232
Six-ring PAHs		4,170	87	69	27	68	30	67	191
Indeno[1,2,3-*c,d*]pyrene	Inp	2,320	46	44	18	35	28	53	106
Benzo[*g,h,i*]perylene	BghiP	1,850	41	25	8.8	33	2.7	14	85
Sum	T-PAHs	10,450	519	309	102	303	259	435	744
Organic content (%)		8.29	7.18	4.30	1.30	4.70	2.80	6.19	5.37
Per_{ANT}		245	4.9	4.3	1.2	2.2	0.4	3.3	3.9
Per_{NAT}		736	155	31	10	24	19	164	228
Per_{ANT} ratio (%)		25	3.1	12	11	8.7	2.3	2.0	1.7

Compound	Abbr.	Concentration (ng/g dry)					
		Site 9	Site 10	Site 11	Site 12	Site 13	Site 14
Naphthalene	Nap	0.6	<0.1	0.4	0.4	1.4	<0.1
Three-ring PAHs		17.8	6.9	9.4	30.8	137	0.6
Acenaphthylene	Acy	1.1	0.3	0.7	1.7	12	<0.1
Acenaphthene	Ace	0.2	<0.1	0.3	1.1	2.0	<0.1
Fluorene	Flu	1.1	<0.1	0.4	2.2	5.2	<0.1
Phenanthrene	Phe	14	5.9	6.9	25	111	0.4
Anthracene	Ant	1.6	0.8	1.1	1.2	7.5	0.2
Four-ring PAHs		127	43.7	92.1	109	788	1.3
Fluoranthene	Flt	30	12	22	33	219	0.5
Pyrene	Pyr	26	9.9	19	29	170	0.8
Benz[*a*]anthracene	BaA	<0.3	<0.3	3.0	<0.3	9.7	<0.3
Chrysene	Chr	22	4.7	17.4	11	154	<0.2
Benzo[*c*]phenanthrene	BcP	48	17	31	36	236	<0.9
Five-ring PAHs[a]		81	47	94	100	494	153
Benzo[*b*]fluoranthene + Benzo[*j*]fluoranthene + Benzo[*k*]fluoranthene	BFs	28	29	25	23	126	38
Benzo[*a*]pyrene	BaP	33	3.2	23	26	185	13

Table 1 continued

Compound	Abbr.	Concentration (ng/g dry)					
		Site 9	Site 10	Site 11	Site 12	Site 13	Site 14
3-Methylcholanthrene	3Mc	<0.8	<0.8	15	11	45	67
Dibenz[*a,h*]anthracene	DahA	20	15	31	40	138	35
Perylene	Per	253	108	105	84	104	86
Six-ring PAHs		107	41	103	148	549	74
Indeno[1,2,3-*c,d*]pyrene	Inp	55	26	54	82	315	36
Benzo[*g,h,i*]perylene	BghiP	52	15	49	66	234	38
Sum	T-PAHs	586	246	404	473	2,070	314
Organic content (%)		5.51	2.66	3.04	3.42	3.12	1.40
Per_{ANT}		5.0	0.5	3.4	4.0	28	1.9
Per_{NAT}		248	107	102	80	77	84
Per_{ANT} ratio (%)		2.0	0.4	3.2	4.7	27	2.2

[a] Total concentrations of five-ring PAHs except for perylene

71 for *n*-alkanes, 136 for naphthalene-d_8 (Nap-d_8), 188 for phenanthrene-d_{10} (Phe-d_{10}), 212 for pyrene-d_{10} (Pyr-d_{10}), 264 for perylene-d_{12} (Per-d_{12}), and 243 for 9-bromoanthracene. The PAHs and *n*-alkanes were determined using the internal standard method. The PAH concentrations were adjusted for the recovery efficiencies of the surrogate compounds. The overall recoveries and relative standard deviations for the surrogate compounds were 32% and 22% for Nap-d_8, 65% and 26% for Phe-d_{10}, 65% and 17% for Pyr-d_{10}, and 80% and 13% for Per-d_{12}, respectively. The concentrations were calculated on a dry basis.

Results and Discussion

The PAH concentrations in the sediment are summarized in Table 1. The total concentrations of the PAHs (T-PAHs) ranged from 102 ng/g at site 4 to 10,450 ng/g at site 1. Site 1 is at a port located on the mouth of the river. Therefore, it was mainly contaminated by emissions from ships. Site 13, which had the second highest T-PAHs, is located at an urban and industrial area with textile factories and dye works factories; site 8, the third highest site, is located at 15 km downstream of an urban area and metalworking factories. Therefore, sites 13 and 8 were contaminated by emissions from the manufacturing plants. The detected compounds showed their characteristic compositions at each site. The four-ring PAHs were the major compounds at site 14; the five-ring PAHs except for Per and six-ring PAHs were the major compounds at sites 5, 6 and 13, and sites 1 and 12, respectively. Therefore, the sediments reflected the local contaminations around and upstream of the investigated sites (Kawata et al. 2005). Per was the major at sites 7, 9 and 10. As described later, Per in the sediment could be derived from natural sources as well as anthropogenic ones (Kawata et al. 1997).

Per was evaluated for its characteristic distribution by comparison with BaP, which originated from anthropogenic sources. The ratio of Per to BaP was compared to the ratio of BaP to the T-PAHs. The Per/BaP ratio in the sediment significantly decreased at $p < 0.01$ with the increasing BaP/T-PAHs ($r = -0.793$). Hence, the Per in the sediment samples originated not only from the same anthropogenic sources as BaP, but also from the natural sources as previously reported (Cranwell and Koul 1989). The anthropogenically derived Per in the sediment was estimated using the Per to BaP ratios in airborne particulate matter (Kawata et al. 1997). The anthropogenic Per in the sediment, Per_{ANT}, was calculated by the following Eq. (1):

$$Per_{ANT} = BaP \times (Per/BaP)_{APM} \quad (1)$$

where BaP is the BaP concentration in the sediment, and $(Per/BaP)_{APM}$, 0.15, is the mean of the relative Per ratio to BaP in the airborne particulate matter in Niigata (Kawata et al. 1997). The naturally derived Per, Per_{NAT}, was calculated by subtracting the Per_{ANT} from the Per concentration. The obtained Per_{ANT} and Per_{NAT} values are listed in Table 1. The percent Per_{ANT} ratios were relatively high (25% and 27%) at sites 2 and 13, respectively, whereas those at the other sites were low (0.4% at site and 10%–12% at site 3). The mean values of the percentile Per_{ANT} in this study were 4.2% geometric and 7.5% arithmetic, which were lower than those (7.8% and 20%, respectively) of 80 sediments from the rivers and the coast of Niigata (Kawata et al. 1997).

The *n*-alkane concentrations in the sediments are summarized in Table 2. The total concentrations of the *n*-alkanes (T-Cs) ranged from 160 ng/g at site 6 to 3,530 ng/g

Table 2 *n*-Alkane concentrations, MCN and CPI values in sediments of the Shinano River

Compound	Abbr.	Concentration (ng/g dry)							
		Site 1	Site 2	Site 3	Site 4	Site 5	Site 6	Site 7	Site 8
Decane	C_{10}	<0.2	<0.2	7.4	5.3	7.5	6.6	2.3	18
Undecane	C_{11}	<0.2	<0.2	1.3	1.5	3.1	<0.2	14	16
Dodecane	C_{12}	9.8	14	1.6	2.8	14	<0.2	8.7	15
Tridecane	C_{13}	<0.1	10	1.4	0.4	<0.1	<0.1	31	52
Tetradecane	C_{14}	30	37	1.7	3.0	40	<0.1	21	48
Pentadecane	C_{15}	4.8	12	3.3	5.5	25	7.5	12	15
Hexadecane	C_{16}	23	33	0.3	2.0	31	<0.3	21	59
Heptadecane	C_{17}	83	57	1.5	5.9	39	<0.2	<0.2	93
Octadecane	C_{18}	90	33	1.1	6.3	38	<0.1	42	61
Nonadecane	C_{19}	22	13	1.5	3.5	16	<0.1	22	32
Eicosane	C_{20}	23	5.8	1.6	5.2	9.2	<0.2	15	8.8
Heneicosane	C_{21}	25	18	1.2	4.7	13	<0.2	17	13
Docosane	C_{22}	19	16	1.6	5.8	15	2.2	27	7.6
Tricosane	C_{23}	27	41	2.4	9.2	14	1.8	34	15
Tetracosane	C_{24}	21	23	6.0	18	32	3.0	38	12
Pentacosane	C_{25}	11	14	3.0	11	14	0.8	10	4.7
Hexacosane	C_{26}	82	131	41	110	82	26	133	27
Heptacosane	C_{27}	139	265	34	91	59	19	203	104
Octacosane	C_{28}	191	190	54	168	35	12	215	54
Nonacosane	C_{29}	395	493	102	256	138	45	399	182
Triacontane	C_{30}	264	215	81	217	39	11	286	61
Hentriacontane	C_{31}	249	529	81	183	154	23	435	163
Dotriacontane	C_{32}	141	157	46	140	35	2.0	252	47
Sum	T-Cs	1,850	2,310	476	1,250	852	160	2,240	1,110
$\Sigma(C_{11}–C_{19})_{ODD}$		110	93	9.0	17	84	7.5	80	208
$\Sigma(C_{12}–C_{20})_{EVEN}$		176	124	6.2	19	131	<0.8	107	192
$\Sigma(C_{21}–C_{31})_{ODD}$		845	1,361	224	555	392	90	1,100	482
$\Sigma(C_{22}–C_{32})_{EVEN}$		718	732	229	658	238	56	951	209
MCN		27	28	28	29	25	27	28	24
CPI		1.07	1.70	0.99	0.84	1.29	1.72	1.11	1.72

Compound	Abbr.	Concentration (ng/g dry)					
		Site 9	Site 10	Site 11	Site 12	Site 13	Site 14
Decane	C_{10}	<0.2	<0.2	<0.2	0.4	0.5	2.6
Undecane	C_{11}	<0.2	<0.2	<0.2	0.9	11	13
Dodecane	C_{12}	23	7.1	15	9.8	15	23
Tridecane	C_{13}	22	8.1	12	13	34	42
Tetradecane	C_{14}	60	18	42	30	43	65
Pentadecane	C_{15}	27	1.5	11	8.5	14	5.3
Hexadecane	C_{16}	45	7.4	28	22	34	52
Heptadecane	C_{17}	115	15	71	59	58	32
Octadecane	C_{18}	45	6.2	25	20	35	30
Nonadecane	C_{19}	27	6.6	16	11	22	21
Eicosane	C_{20}	10	<0.2	9.5	5.0	6.9	3.5
Heneicosane	C_{21}	20	5.2	14	10	12	4.1
Docosane	C_{22}	18	4.2	12	10	9.0	0.9
Tricosane	C_{23}	44	4.1	27	23	19	0.6

Table 2 continued

Compound	Abbr.	Concentration (ng/g dry)					
		Site 9	Site 10	Site 11	Site 12	Site 13	Site 14
Tetracosane	C_{24}	39	4.0	19	24	15	<1
Pentacosane	C_{25}	20	2.3	10	13.4	12	0.2
Hexacosane	C_{26}	108	25	68	122	68	0.7
Heptacosane	C_{27}	429	61	241	330	312	7.7
Octacosane	C_{28}	202	77	152	297	158	10
Nonacosane	C_{29}	708	148	378	636	670	20
Triacontane	C_{30}	245	168	168	495	305	16
Hentriacontane	C_{31}	690	139	354	734	1,350	17
Dotriacontane	C_{32}	177	64	134	400	324	9 .0
Sum	T-Cs	3,070	772	1,810	3,270	3,530	377
$\Sigma(C_{11}–C_{19})_{ODD}$		191	31	110	92	139	114
$\Sigma(C_{12}–C_{20})_{EVEN}$		182	39	120	86	134	174
$\Sigma(C_{21}–C_{31})_{ODD}$		1,910	361	1,020	1,750	2,370	50
$\Sigma(C_{22}–C_{32})_{EVEN}$		789	341	553	1,350	879	37
MCN		27	28	27	29	29	18
CPI		2.17	1.03	1.69	1.28	2.48	0.77

at site 13. The T-PAHs at site 1 was 24 and 26 times the concentrations at sites 7 and 11, respectively (Table 1). In contrast, the T-Cs at site 1 was almost the same as that at site 11 and 83% of that at site 7. Moreover, the ratios of the T-PAHs at sites 3, 4 and 5, which are located within 2 km of each other, were 3.0:1.0:3.0 (Table 1), while the ratios of the T-Cs were 0.38:1.0:0.68. Therefore, the origins of the *n*-alkanes in the sediments could differ from those of the PAHs. The *n*-alkanes, except for C_{10}, were classified into four groups according the carbon numbers of the *n*-alkanes, $(C_{11}–C_{19})_{ODD}$, $(C_{12}–C_{20})_{EVEN}$, $(C_{21}–C_{31})_{ODD}$ and $(C_{22}–C_{32})_{EVEN}$, where $(C_i–C_j)_{ODD}$ and $(C_i–C_j)_{EVEN}$ are the concentrations of the *n*-alkane with odd and even carbon numbers, respectively, over the range *i*–*j*. The total concentrations of each group are listed in Table 2. Although the compositions of the four *n*-alkane groups were characteristic at each site, $\Sigma(C_{21}–C_{31})_{ODD}$ was the major compounds except for sites 3, 4, and 14. $\Sigma(C_{12}–C_{20})_{EVEN}$ was predominant at site 14, while $\Sigma\ (C_{22}–C_{32})_{\ EVEN}$ was the major compounds at sites 3 and 4. The mean carbon number (MCN) of the *n*-alkanes in the sediment samples was calculated according to the following Eq. (2):

$$\mathrm{MCN} = \sum (i \times [\mathrm{C}_i]) \Big/ [\mathrm{T\text{-}C_s}] \qquad (2)$$

where $[C_i]$ and [T-Cs] are the concentration of the *n*-alkane with carbon number i and that of the T-Cs, respectively. The MCN values (Table 2) at sites 5, 8 and 14 were 18–25, whereas those at the other sites were 27–29. The low MCN values could be ascribed to the high relative abundance of trees compared to grasses and herbs during the low flux of organic carbon (Tareq et al. 2005). The carbon preference index (CPI) has been used to estimate the source of the *n*-alkanes. The CPI values for the petroleum were reported to be 0.93–1.07 (Zdanaviciute et al. 2007). On the other hand, the CPI values for plants were reported to be 2.3–54.3 (Bi et al. 2005). Therefore, CPI values close to unity indicate the greater contribution of *n*-alkanes from artificial sources, e.g., biomass burning, and petroleum pollution; higher CPI values indicate a higher contribution from natural sources, e.g., terrestrial vegetation and biogeneic (Tareq et al. 2005). The CPI was calculated using the following Eq. (3):

$$\mathrm{CPI} = \sum (\mathrm{C}_{11} - \mathrm{C}_{31})_{\mathrm{ODD}} \Big/ \sum (\mathrm{C}_{12} - \mathrm{C}_{32})_{\mathrm{EVEN}} \qquad (3)$$

where $(C_i–C_j)_{ODD}$ and $(C_i–C_j)_{EVEN}$ are the concentrations of the *n*-alkane with an odd carbon number and that with an even carbon number, respectively, over the range i–j. The calculated CPI values are given in Table 2. The CPI values at sites 9 and 13 were >2.0. Therefore, the natural sources could contribute to the *n*-alkanes at these sites. On the other hand, the CPI at sites 1, 3, 4, 7 and 10 were within 1.00 ± 0.20. Thus the artificial sources could predominantly contribute to the *n*-alkanes. Moreover, the CPI at site 14 was 0.77, which most approximates the CPI at site 4. However, the *n*-alkane compositions at these sites were markedly different, and the MCN at site 14 (18) was quite lower than that at site 4 (29). This indicates that the artificial sources at site 14 were different from those at site 4. In addition, Tareq et al. (2005) reported that the CPI correlated with the MCN in sediments from Indonesia.

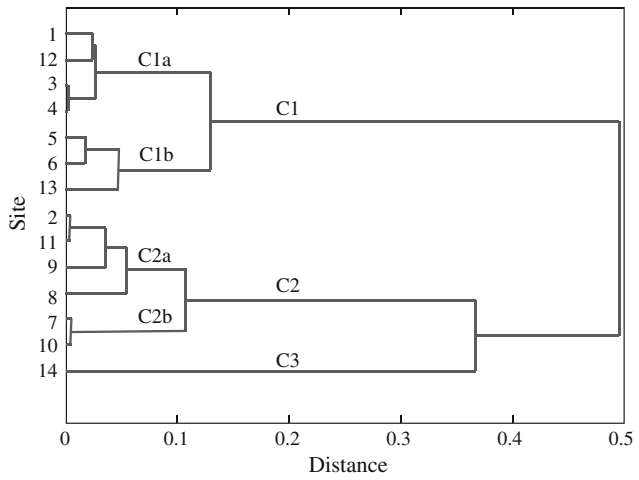

Fig. 2 Dendrogram of cluster analysis by Ward's method

However, the MCN did not significantly correlate with the CPI in our study. This indicates the differences in the *n*-alkane sources at both investigated sites.

The similarity in the distribution patterns of the PAHs and *n*-alkanes from the sampling sites was compared using the cluster analysis. Among the PAHs, BaP and Per were selected, because the BaP concentration significantly correlated with those of the most anthropogenic PAHs, and Per has both anthropogenic and natural sources. $\Sigma(C_{21}–C_{31})_{ODD}$ and $\Sigma(C_{22}–C_{32})_{EVEN}$ were used for the cluster analysis, because the distributions of the *n*-alkanes were represented by the total concentrations of the *n*-alkanes with odd carbon numbers and those with even carbon numbers, and the *n*-alkanes with 21–31carbons were the predominant ones at most sites. To avoid the effect of the concentration levels, all the variables were divided by the total concentrations. Namely, BaP/T-PAH, Per/T-PAH, $\Sigma(C_{21}–C_{31})_{ODD}$/T-Cs and $\Sigma(C_{22}–C_{32})_{EVEN}$/T-Cs were used for the cluster analysis. Each variable was standardized to a mean of 0 and standard deviation of 1. Ward's method was used as the algorithm of the analysis. The obtained dendrogram is shown in Fig. 2. Sites 1–14 were divided into three clusters (C1–C3). C1 contained seven sites with relatively low Per compositions, whereas C2 and C3 contained the sites with relative high Per compositions. Moreover, the percent Per_{ANT} ratios were 4.7%–27% and 0.4%–3.2% in C1 and the other clusters, respectively. Therefore, the sites in C1 could be affected by anthropogenic sources compared to the sites in C2 and C3; site 14 (C3) was a unique point with the lowest MCL and CPI of the investigated sites described above. C1 consisted of two semiclusters (C1a and C1b); the sites in C1a had higher BaP, Per and $\Sigma(C_{22}–C_{32})_{EVEN}$ compositions, and lower CPI values than the sites in C1b. This suggests that the former sites could be affected by the anthropogenic sources more than the latter sites. Similarly, C2 consisted of two semiclusters (C2a and C2b); the sites in C2b had higher $\Sigma(C_{22}–C_{32})_{EVEN}$ compositions and lower CPI values (close to unity) than the sites in C2a, suggesting that the former sites could be affected by the anthropogenic sources more than the latter sites. Consequently, the clusters could be characterized by the four variables.

References

Bi X, Sheng G, Liu X, Li C, Fu J (2005) Molecular and carbon and hydrogen isotopic composition of *n*-alkanes in plant leaf waxes. Org Geochem 36:1405–1417. doi:10.1016/j.orggeochem.2005.06.001

Cranwell PA, Koul VK (1989) Sedimentary record of polycyclic aromatic and aliphatic hydrocarbons in the Windemere catchment. Water Res 23:275–283. doi:10.1016/0043-1354(89)90092-4

Kawata K, Tanabe A, Mitobe H, Sakai M, Yasuhara A (1997) Distribution of perylene and five-ring polycyclic aromatic hydrocarbons in sediment and airborne particulate matter. Toxicol Environ Chem 63:97–106. doi:10.1080/02772249709358520

Kawata K, Tanabe A, Asada T, Oikawa K (2005) Distribution of semivolatile cyclic compounds in sediment from Niigata, Japan. Bull Environ Contam Toxicol 75:546–553. doi:10.1007/s00128-005-0786-9

Tareq SM, Tanoue E, Tsuji H, Tanaka N, Ohta K (2005) Hydrocarbon and elemental carbon signatures in a tropical wetland: biogeochemical evidence of forest fire and vegetation changes. Chemosphere 59:1655–1665. doi:10.1016/j.chemosphere.2005.02.019

Vrana B, Paschke A, Popp P (2001) Polyaromatic hydrocarbon concentrations and patterns in sediments and surface water of the Mansfeld region, Saxony-Anhalt, Germany. J Environ Monit 3:602–609. doi:10.1039/b104707h

Ye B, Zhang Z, Mao T (2007) Petroleum hydrocarbon in surficial sediment from rivers and canals in Tianjin, China. Chemosphere 68:140–149. doi:10.1016/j.chemosphere.2006.12.074

Zdanaviciute O, Dakhnova MV, Zheglova TP (2007) Geochemistry of oil and source rocks and petroleum potential of the western part of Baltic Syneclise. Abstract 15th Meet Assoc European Geolog Soc 82–83